A new deep-branching stramenopile, *Platysulcus tardus* gen. nov., sp. nov.

Takashi Shiratori[a], Takeshi Nakayama[b], and Ken-ichiro Ishida[b,1]

[a]Graduate School of Life and Environmental Sciences, University of Tsukuba, Tsukuba, Ibaraki 305-8572, Japan;

[b]Faculty of Life and Environmental Sciences, University of Tsukuba, Tsukuba, Ibaraki 305-8572, Japan

Running title: A new deep-branching stramenopile

[1] Corresponding Author: FAX: +81 298 53 4533

E-mail: ken@biol.tsukuba.ac.jp (K. Ishida)

A novel free-living heterotrophic stramenopile, *Platysulcus tardus* gen. nov., sp. nov. was isolated from sedimented detritus on a seaweed collected near the Ngeruktabel Island, Palau. *P. tardus* is a gliding flagellate with tubular mastigonemes on the anterior short flagellum and a wide, shallow ventral furrow. Although the flagellar apparatus of *P. tardus* is typical of stramenopiles, it shows novel ultrastructural combinations that are not applied to any groups of heterotrophic stramenopiles. Phylogenetic analysis using SSU rRNA genes revealed that *P. tardus* formed a clade with stramenopiles with high statistical support. However, *P. tardus* did not form a subclade with any species or environmental sequences within the stramenopiles, and no close relative was suggested by the phylogenetic analysis. Therefore, we concluded that *P. tardus* should be treated as a new genus and species of stramenopiles.

Key words: flagellar apparatus; MAST; phylogenetic analysis; stramenopiles; ultrastructure

Introduction

Stramenopiles are a major eukaryotic assemblage that is characterized by tripartite flagellar hairs (tubular mastigonemes) on the anterior flagellum and a unique flagellar apparatus consisting of four microtubular roots (Andersen 1991; Karpov et al. 2001; Moestrup and Andersen 1991). Stramenopiles consist of photosynthetic and heterotrophic organisms that live in marine, freshwater, and terrestrial environments (Andersen 2004). The photosynthetic stramenopiles are classified into over 10 classes that include well-known groups of large multicellular brown seaweeds (Phaeophyceae) and several unicellular algae (e.g., Bacillariophyceae, Chrysophyceae, and Raphidophyceae). Heterotrophic groups have various morphologies and lifestyles such as phagotrophic flagellates (e.g., Placicidea and Bikosea), fungus-like osmotrophic organisms (e.g., Pseudofungi and Labyrinthulea), and intestinal parasites of animals (e.g., Blastocystea and Opalinea). While phylogenetic analyses have shown that photosynthetic stramenopiles form a monophyletic group, most heterotrophic members are placed in basal lineages and the detailed phylogenetic position of each lineage remains uncertain (Cavalier-Smith and Chao 2006; Cavalier-Smith and Scoble 2013; Risers et al. 2009).

Environmental DNA surveys have shown that there are many unidentified lineages of marine stramenopiles (MAST) (e.g., Lin et al. 2012; Massana et al. 2002, 2004, 2014). Sequences from MAST clades have been reported from various marine environments from the upper ocean to anoxic sediment (e.g., Lin et al. 2012; Takishita et al. 2005). Previous studies using in situ fluorescence hybridization methods (FISH) showed that some of these unidentified stramenopiles are relatively small (<10 μm) and bacterivorous (Kolodziej and Stoeck 2007; Massana et al. 2002). In fact, the small heterotrophic flagellates *Solenicola setigera* and *Incisomonas marina* have recently been confirmed to be included in MAST-3 (Cavalier-Smith and Scoble 2013; Gómez et al. 2011). Nevertheless, more than 10

undescribed environmental clades still exist. Revealing the morphology and ultrastructure of these undescribed stramenopiles is important for understanding the diversity and evolution of stramenopiles.

In this study, we established a culture of a small bacterivorous flagellate (strain SRT153). In phylogenetic analysis using the small subunit ribosomal RNA (SSU rRNA) gene, the flagellate formed a monophyletic group with stramenopiles with high statistical support, however, it branched as a distinct lineage from any known stramenopiles or environmental sequences. We also performed light and electron microscopic observations on this flagellate, and these provided useful information for discussing the taxonomic position of the strain.

Results

Light microscopy

Cells of *Platysulcus tardus* gen. nov., sp. nov. were oval or ovoid with a length of 5.62 (3.6–7.8) μm and width of 3.76 (3.1–4.5) μm (n = 41) (Fig. 1A–E). Thecae or scales were not observed on the surface of the cell. Cells often contained oval or rod-like contents that were considered to be captured bacteria (Fig. 1B). A wide, shallow ventral furrow was located at the ventral side of the cell (Fig. 1C–E). Two flagella were inserted in the anterior end of the ventral furrow; the short anterior flagellum (about 9 μm, n = 32) was directed anteriorly and the long posterior flagellum (about 17 μm, n = 33) was directed posteriorly (Fig. 1B–E). Most cells in the culture showed slow gliding motion. When the cell was gliding, the anterior flagellum showed rapid sinusoidal waves and the posterior flagellum trailed posteriorly and was attached to the substratum. In the aged culture, swimming cells were frequently observed. Cells swam slowly with a wobbling and spiral motion. Neither cysts nor a multinucleate stage were observed.

Transmission electron microscopy

Whole-mount observation showed that cells had a short anterior flagellum with tubular mastigonemes and a long naked posterior flagellum (Fig. 1F, G). The mastigonemes were composed of at least two parts, a short shaft and a long terminal filament (Fig. 1G, H). Neither flagellum was acronematic (Fig. 1F).

In ultra-thin section observation, cells were covered only by a plasma membrane and no additional structures were observed on the surface of the cell (Fig. 2A, E). Cells had one nucleus with one conspicuous nucleolus (Fig. 2A). The nucleus was located anterior to the middle part of the cell, and connected to a well-developed rough endoplasmic reticulum (ER) (Fig. 2A). Thin, fibrous materials were observed in the ER, which probably corresponded to the mastigonemes on the anterior flagellum (Fig. 2B). Several roundish

mitochondrial profiles with tubular cristae were scattered around the nucleus (Fig. 2A). A Golgi apparatus was located anterior to the nucleus (Fig. 2A). Several small globular microbodies were observed around the nucleus (Fig. 2C). Food vacuoles containing digested bacteria were occasionally observed in the cytoplasm (Fig. 2D, 5A–E). Electron-dense extrusomes were located just beneath the plasma membrane, especially along the ventral side of the cell (Fig. 2E). The extrusomes were roundish and approximately 200 nm in diameter, and contained a cylindrical structure (Fig. 2E). The cytoplasm containing a nucleus, mitochondria, and microbodies was surrounded by a large flat vesicle, whereas the food vacuoles and extrusomes were not (Fig. 2A, 4, 5). The flat vesicle did not enclose the cytoplasm completely but exhibited some gaps such as the position facing the Golgi body and basal bodies (Fig. 2A).

The middle region of basal bodies was filled with electron-dense material (Fig. 2F, H). A short cartwheel structure was observed at the proximal end of the basal body (Fig. 2G). The cartwheel structure was less dense and was difficult to be recognized in longitudinal sections. A dense plate was observed at the flagellar transitional region (Fig. 2F, I). No additional ring-shaped or helical structures, such as a transitional helix, spiral fiber, or intrakinetosomal shelves, were observed in the transitional region or basal body (Fig. 2F–J). The anterior and posterior basal bodies were arranged at a right angle (Fig. 3). They were not in the same plane, and the right side of the posterior basal body was closely associated with the left side of the anterior basal body (Fig. 3, 5).

To describe the microtubular roots of *P. tardus*, we applied the terminology in Moestrup (2000). The posterior basal body had three microtubular roots. Root 2 (R2) emerged from the right side of the posterior basal body. The base of the R2 consisted of 11 microtubules that were aligned in an “L”-shape (Fig. 3D, E). We numbered each microtubule of R2 as described in Moestrup and Thomsen (1976) (1–8 and a–c, from right

to left). The microtubules of the R2 were split into two rows, and the number of microtubules gradually decreased from the middle part. Microtubules 5, 6, and 7 of the R2 initially disappeared and the R2 was split into inner (8, a–c,) and outer (1–4) rows (Fig. 3F, G), and, finally, each row decreased into a single microtubule (Fig. 4E, F, 5A, B). Each row of R2 ran just beneath the ventral surface and supported the right side of the ventral furrow (Fig. 5). Root 1 (R1) consisted of three or four microtubules and emerged from the left anterior side of the posterior basal body (Fig. 3C–H, 4, 5B–D). The R1 ran just beneath the ventral surface and supported the left side of the ventral furrow (Fig. 3C–H, 4, 5B–D). The S tubule consisted of a single, short microtubule that emerged from the posterior side of the posterior basal body (Fig. 3B–G, 4A–C, 5A–D). The S tubule joined together with the R1 and supported the anterior part of the left side of the ventral furrow (Fig. 3B–G, 4A–C, 5A–D). The anterior basal body had two microtubular roots. Root 3 (R3) emerged from the right side of the anterior basal body and went towards the dorsal side of the cell (Fig. 5C–F). The R3 consisted of two microtubules (Fig. 5C–F). Root 4 (R4) emerged from the opposite side of the R3 and ran parallel to the R3 (Fig. 5B–D). The R4 consisted of one microtubule (Fig. 5B–D). The microtubular roots are illustrated in Figure 6.

Phylogenetic analysis

We sequenced almost the complete length of the SSU rRNA gene of *P. tardus* (1786 bp). No intron was confirmed in the sequence. Our phylogenetic analysis, including all major taxonomic groups and environmental clades of stramenopiles, showed that *P. tardus* branched as a sister lineage of a clade of stramenopiles, and the monophyly of *P. tardus* and stramenopiles was strongly supported (Fig. 7). However, statistical support for the monophyly of stramenopiles, except for *P. tardus*, was weak, and the phylogenetic position of *P. tardus* within stramenopiles was unsolved.

Discussion

Our molecular phylogenetic analysis using the SSU rRNA gene showed that *Platysulcus tardus* gen. nov., sp. nov. was included in the stramenopiles with high statistical support (bootstrap probability = 89%, Bayesian posterior probability = 1.00). In the ML tree, *P. tardus* branched as the most basal lineage of stramenopiles. However, the phylogenetic analysis could not reveal the detailed phylogenetic position of *P. tardus* within stramenopiles. Interestingly, *P. tardus* did not form a subclade with any known species or MAST environmental sequence, which suggests that *P. tardus* represents a novel lineage that has never been detected, even by the environmental DNA survey. Microscopic observations showed that *P. tardus* has shared characteristics of stramenopiles, namely tubular mastigonemes on the anterior flagellum and four major microtubular roots (R1–R4). On the other hand, the general morphology and the flagellar apparatus of *P. tardus* can be distinguished from known stramenopiles.

Light microscopic observation showed that *P. tardus* exhibit slow gliding movement with the long, trailing posterior flagellum. Although gliding movement is common in several groups of heterotrophic protists (e.g., Cercozoa, Apusozoa, and Euglenozoa), it is relatively rare in stramenopiles. Placididea, a known group of gliding stramenopiles, includes two species (*Placidia cafeteriopsis* and *Wobblia lunata*). However, both species have a long anterior flagellum and a short posterior flagellum (Moriya et al. 2000, 2002), whereas *P. tardus* has a short anterior flagellum and a long posterior flagellum. *Incisomonas marina* is a nanomonadean gliding flagellate, but it is different from *P. tardus* and most stramenopiles in only having a naked posterior flagellum (Cavalier-Smith and Scoble 2013). The bikosean *Caecitellus parvulus* is also a gliding heterotrophic stramenopile with a short anterior flagellum and a long posterior flagellum. However, *C. parvulus* lacks mastigonemes on the anterior flagellum (O'Kelly and Nerad 1998). In

addition, *P. tardus* is also distinguishable from these gliding heterotrophic stramenopiles in having a wide ventral furrow.

The flagellar apparatus is one of the most significant taxonomic traits for the higher classification of stramenopiles (Andersen 1991, Cavalier-Smith and Chao 2006,). Helical structures in the flagellar transitional region or basal bodies are widely observed among stramenopiles, although *P. tardus* lacks these structures. A single transitional helix in the flagellar transitional region has been reported in various groups of Ochrophyta, such as Chrysophyceae and Eustigmatophyceae, but some xanthophyceans have a double transitional helix and several groups (e.g., Bolidophyceae, Phaeophyceae, and Raphidophyceae) lack these structures (Andersen 2004; Cavalier-Smith and Chao 2006; Preisig 1989). Pseudofungi (oomycetes, hyphochytrids, and *Developayella*) usually have a double transitional helix (Barr and Désaulniers 1989; Beakes et al. 2012; Cavalier-Smith 1997). The early divergent stramenopiles Placididea and Opalinea also have a double transitional helix just above the transitional plate (Cavalier-Smith 1997; Cavalier-Smith and Chao 2006; Moriya et al. 2002; Patterson 1985; Patterson and Delvinquier 1990). Placididea and Opalinea additionally have a spiral structure (intrakinetosomal shelves) in the basal body (Moriya et al. 2002; Patterson 1985). Labyrinthulea have a bell-shaped structure in the transitional region (Barr and Allan 1985). Some bikosean flagellates have a spiral fiber (e.g., *Adriamonas peritocrescens*, *Bicosoeca maris*, and *Boroka karpovii*), or intrakinetosomal shelves (e.g., *Rictus lutensis*), while most species lack these structures like *P. tardus* (Cavalier-Smith and Chao 2006; Karpov et al. 2001; Yubuki et al. 2010).

The microtubular roots of *P. tardus* are similar to those of typical stramenopiles, especially Bikosea and Placididea. Typical bikosean flagellates have an “L”-shaped R2 consisting of 8+3 microtubules like *P. tardus*, and several species also have an S tubule (e.g., *Bicosoeca maris*, *Boroka karpovii*, and *Rictus lutensis*) (Karpov et al. 2001; Moestrup

and Thomsen 1976; Yubuki et al. 2010). However, *P. tardus* is different from Bikosea in the absence of a single microtubule that is associated with R2 (x fiber). The x fiber is reported in all orders in Bikosea and is regarded as one of the taxonomic traits of this class (Cavalier-Smith and Chao 2006; Karpov et al. 2001). The placididean flagellate lacks x fiber, the same as *P. tardus* (Moriya et al. 2000, 2002). However, in contrast to *P. tardus*, placidians lack the S tubule and their R2 consists of 7+3 microtubules arranged in a "U"-shape (Moriya et al. 2000, 2002).

These light and electron microscopic observations revealed that there are no stramenopiles that show strong morphological affinity with *P. tardus*. Additionally, we also confirmed that *P. tardus* can be distinguished from gliding flagellates with uncertain taxonomic positions or without molecular and ultrastructural data (e.g., *Glissandra*, *Kiitoksia*, and *Pseudophyllomitus*) (Lee 2002; Patterson and Simpson 1996; Vørs 1992) by the combination of general morphological features such as cell shape and size, flagellar length, and presence of a wide ventral furrow. Therefore, we concluded that *P. tardus* is a new genus and species of stramenopiles. Our phylogenetic analysis showed that *P. tardus* does not form a subclade with any available sequences. Characteristics of the flagellar apparatus of *P. tardus* also did not correspond with any classes or orders of stramenopiles. Therefore, we treated *P. tardus* as stramenopiles incertae sedis.

Taxonomic treatment

Platysulcidae fam. nov. Shiratori, Nakayama, and Ishida (ICZN)

Description: Phagotrophic biflagellates with tubular mastigoneme on anterior flagellum. Cells with mitochondria with tubular cristae. Basal body and flagellar transitional region lacking ring-shaped or helical structures. Cells with S tubule but without x fiber. Root 2 consisting of 11 microtubules and aligning "L"-shape at its origin.

Type genus: *Platysulcus*.

Platysulcus gen. nov. Shiratori, Nakayama, and Ishida (ICZN)

Description: Marine bacterivorous flagellates with short anterior flagellum and long posterior flagellum. Cells with wide, shallow ventral furrow. Cells showing slow gliding movement.

Type species: *Platysulcus tardus*.

Etymology: The genus name "*Platysulcus*" derived from the Latin *platy* (wide) and *sulcus* (furrow), referring to the wide ventral furrow of the cell. *Platysulcus* is considered to be of male gender

Platysulcus tardus sp. nov. Shiratori, Nakayama, and Ishida (ICZN)

Description: Cells oval or ovoid, 5.62 (3.6–7.8) μm in length and 3.76 (3.1–4.5) μm in width. Anterior flagellum about 9 μm and posterior flagellum about 17 μm in length. Extrusomes present. Large, flat vesicle surrounding cytoplasm containing a nucleus, mitochondria, and microbodies.

Hapantotype: One monoclonal culture used for describing this study (NIES-3720), deposited and maintained at the National Institute for the Environmental Sciences, Tsukuba.

Paratype: One microscope slide (TNS-AL-58905S) and one EM block (TNS-AL-58905TB), deposited in the herbarium of the National Museum of Nature and Science (TNS), Tokyo. These cells are derived from the same sample as the holotype.

DNA sequence: Small subunit ribosomal DNA, LC028904.

Type locality: Sedimented detritus on seaweed, Ngeruktabel Island, Republic of Palau (latitude = 7.2545, longitude = 134.4444).

Collection date: November 11, 2011.

Etymology: Specific epithet “*tardus*” (slow, late) refers to the slow gliding movement of the cell.

Methods

Culture establishment

We collected a sample of sedimented detritus on seaweeds at the Ngeruktabel Island, Palau on November 11, 2011 (latitude = 7.2545, longitude = 134.4444). A sufficient volume of ESM medium (Kasai et al. 2009) was added to the sample and kept at 20°C under a 14-h light/10-h dark cycle for initial cultivation. A culture of *Platysulcus tardus* gen. nov., sp. nov. (strain SRT153) was established using a single-cell isolation technique from the enriched sample. The culture was cultivated with ESM medium and contaminant bacteria as a food source and kept at 20°C under dark conditions. The strain SRT153 was deposited at the National Institute for the Environmental Sciences, Tsukuba as NIES-3720.

Light and electron microscopy

The cells of the strain SRT153 were observed using an Olympus IX71 inverted microscope (Olympus, Tokyo, Japan) equipped with an Olympus DP71 CCD camera (Olympus).

For the observation of whole-mount cells under TEM, cell suspensions were mounted on formvar-coated copper grids and fixed by OsO_4 vapor. The copper grids were washed with distilled water and stained with 2% (w/v) uranyl acetate and observed using a Hitachi H-7650 electron microscope (Hitachi High-Technologies Corp., Tokyo, Japan) equipped with a Veleta TEM CCD camera (Olympus Soft Imaging System, Munster, Germany).

A specimen for ultra-thin section observation using transmission electron microscopy was prepared as follows: pellets of centrifuged cells were placed on a formvar-coated copper loop and plunged rapidly into liquid propane. The frozen pellets were plunged into liquid nitrogen for several seconds and placed in a mixture of 0.1% glutaraldehyde and 2% osmium tetroxide in acetone at -80°C for 48 h. Then, the fixing solution was kept at -20°C for 2 h, and -4°C for 2 h. The pellets were rinsed with acetone

three times and replaced by Agar Low Viscosity Resin R1078 (Agar Scientific Ltd, Stansted, England). The resin was polymerized by heating at 60°C for 8 h. Ultrathin sections were prepared on a Reichert Ultracut S ultramicrotome (Leica, Vienna, Austria), double stained with 2% (w/v) uranyl acetate and lead citrate (Hanaichi et al. 1986; Sato 1968), and observed using a Hitachi H-7650 electron microscope (Hitachi High-Technologies Corp., Tokyo, Japan) equipped with a Veleta TEM CCD camera (Olympus Soft Imaging System, Munster, Germany).

DNA extraction and polymerase chain reaction (PCR): Cells of the strain SRT153 were centrifuged and total DNA was extracted from the pellet using a DNeasy Plant mini kit (Qiagen Science, Valencia, CA), according to the manufacturer's instructions. SSU rRNA of the strain SRT153 was amplified by polymerase chain reaction (PCR) with 18F-18R primers (Yabuki et al. 2010). Amplifications consisted of 30 cycles of denaturation at 94°C for 30 s, annealing at 55°C for 30 min, and extension at 72°C for 2 min. An additional extension for 4 min at 72°C was performed at the end of the reaction. Amplified DNA fragments were purified after gel electrophoresis with a QIAquick Gel Extraction Kit (Qiagen Science), and then cloned into the p-GEM® T-easy vector (Promega, Tokyo, Japan). The inserted DNA fragments were completely sequenced by a 3130 Genetic Analyzer (Applied Biosystems, Monza, Italy). The SSU rDNA sequence of the strain SRT153 is deposited as LC028904 in GenBank.

Sequence alignments and phylogenetic analysis: We newly created the SSU rDNA alignment set of stramenopiles, and the SSU rDNA sequence of the strain SRT153 was added to this alignment set. The sequences of the alignment set were automatically aligned with MAFFT (Katoh and Toh 2008) and then edited manually with SeaView (Galtier et al. 1996). For phylogenetic analysis, ambiguously aligned regions were manually deleted from each alignment. Finally, we prepared SSU rDNA alignment (1,607 positions). The

alignment file that was used in the analysis is available on request. The maximum likelihood (ML) tree was heuristically searched using RAxML v.7.2.6 (Stamatakis 2006) under the GTR+Γ model. Tree searches started with 20 randomized maximum-parsimony trees, and the highest log likelihood (lnL) was selected as the ML tree. A non-parametric bootstrap analysis with 1000 replicates was conducted under the GTR+Γ model. A Bayesian analysis was run using MrBayes v. 3.2.2 (Ronquist and Huelsenbeck 2003) with the GTR + Γ model for the same dataset. One cold and three heated Markov chains with default temperature parameter were run for 5×10^6 generations, sampling lnL values and trees at 100-generation intervals. Convergence was assessed by average standard deviation of split frequencies and the first 1×10^6 generations of each analysis were discarded as "burn-in". Bayesian posterior probability and branch lengths were calculated from the remaining trees.

Acknowledgments

We thank the Ministry of Natural Resources, Environment, and Tourism, Palau for providing permits for collecting marine resources (permit number, RE-11-18).We thank Dr. Naoto Hanzawa at Yamagata University for trip management for sampling. This work was supported by JSPS KAKENHI Grant Numbers 13J00587 and 23405013.

References

Andersen RA (1991) The cytoskeleton of chromophyte algae. Protoplasma **164**:143–159

Andersen RA (2004) Biology and systematics of heterokont and haptophyte algae. Am J Bot **91**:1508–1522

Barr DJS, Allan PME (1985) A comparison of the flagellar apparatus in *Phytophthora*, *Saprolegnia*, *Thraustochytrium*, and *Rhizidiomyces*. Can J Bot **63**:138–154

Barr DJS, Désaulniers NL (1989) The flagellar apparatus of the Oomycetes and Hyphochytriomycetes. The Chromophyte Algae: Problems and Perspectives. Syst Assoc Spec **38**:343–355

Beakes GW, Glockling SL, Sekimoto S (2012) The evolutionary phylogeny of the oomycete "fungi". Protoplasma **249**:3–19

Cavalier-Smith T (1997) Sagenista and Bigyra, two phyla of heterotrophic heterokont chromists. Arch Protistenkd **148**:253–267

Cavalier-Smith T, Chao EE (2006) Phylogeny and megasystematics of phagotrophic heterokonts (Kingdom Chromista). J Mol Evol **62**:388–420

Cavalier-Smith T, Scoble JM (2013). Phylogeny of Heterokonta: *Incisomonas marina*, a uniciliate gliding opalozoan related to *Solenicola* Nanomonadea), and evidence that Actinophryida evolved from raphidophytes. Eur J Protistol **49**:328–353

Galtier N, Gouy M (1996) SEAVIEW and PHYLO_WIN: two graphic tools for sequence alignment and molecular phylogeny. Comput Appl Biosci **12**:543–548

Gómez F, Moreira D, Benzerara K, López-García P (2011) *Solenicola setigera* is the first characterized member of the abundant and cosmopolitan uncultured marine stramenopile group MAST-3. Environ Microbiol **13**:193–202

Hanaichi T, Sato T, Hoshino M, Mizuno N (1986) A stable lead stain by modification of Sato's method. Proceedings of the XIth International Congress on Electron Microscopy,

Japanese Society for Electron Microscopy, Kyoto, Japan, pp 2181–2182

Karpov SA, Sogin ML, Silberman JD (2001) Rootlet homology, taxonomy, and phylogeny of bicosoecids based on 18S rRNA gene sequences. Protistology **2**:34–47

Kasai F, Kawachi M, Erata M, Mori F, Yumoto K, Sato M, Ishimoto M (2009) NIES-Collection. List of strains (8th ed.) Jpn J Phycol (Sôrui) **57**:1–350

Katoh K, Toh H (2008) Recent developments in the MAFFT multiple sequence alignment program. Brief Bioinform **9**:286–298

Kolodziej K, Stoeck T (2007) Cellular identification of a novel uncultured marine stramenopile (MAST-12 clade) small-subunit rRNA gene sequence from a Norwegian estuary by use of fluorescence in situ hybridization-scanning electron microscopy. Appl Environ Microbiol **73**:2718–2726

Lee WJ (2002) Redescription of the rare heterotrophic flagellate (Protista) –*Phyllomitus undulans* Stein, 1878, and erection of a new genus– *Pseudophyllomitus* gen. n. Acta Protozool **41**:375–381

Lin YC, Campbell T, Chung CC, Gong GC, Chiang KP, Worden AZ (2012) Distribution Patterns and Phylogeny of Marine Stramenopiles in the North Pacific Ocean. Appl Environ Microbiol **78**:3387–3399.

Massana R, Castresana J, Balague V, Guillou L, Romari K, Groisillier A, Valentin K, Pedros-Alio C (2004) Phylogenetic and ecological analysis of novel marine stramenopiles. Appl Environ Microbiol **70**:3528–3534

Massana R, del Campo J, Sieracki ME, Audic S, Logares R (2014) Exploring the uncultured microeukaryote majority in the oceans: reevaluation of ribogroups within stramenopiles. ISME J. **8**:854–866

Massana R, Guillou L, Diéz B, Pedrós-Alió C (2002) Unveiling the organisms behind novel eukaryotic ribosomal DNA sequences from the ocean. Appl Environ Microbiol

68:4554–4558

Moestrup Ø (2000) The Flagellate Cytoskeleton: Introduction of a General Terminology for Microtubular Roots in Protists. In Leadbeater BS, Green JC (eds) The Flagellates: Unity, Diversity and Evolution. Taylor & Francis, London, pp 69–94

Moestrup Ø, Andersen R (1991) Organization of Heterotrophic Heterokonts. In Patterson DJ, Larsen J (eds) The Biology of Free-living Heterotrophic Flagellates. Oxford University Press, New York, pp 333–360

Moestrup Ø, Thomsen HA (1976) Fine structural studies on the flagellate genus *Bicoeca*. I. *Bicoeca maris* with particular emphasis on the flagellar apparatus. Protistologica **12**:101–120

Moriya M, Nakayama T, Inouye I (2000) Ultrastructure and 18S rDNA sequence analysis of *Wobblia lunata* gen. et sp. nov., a new heterotrophic flagellate (Stramenopiles, Incertae sedis). Protist **151**:41–55

Moriya M, Nakayama T, Inouye I (2002) A new class of the stramenopiles, Placididea Classis nova: description of *Placidia cafeteriopsis* gen. et sp. nov. Protist **153**:143–156

O'Kelly CJ, Nerad TA (1998) Kinetid architecture and bicosoecid affinities of the marine heterotrophic nanoflagellate *Caecitellus parvulus* (Griessmann, 1913) Patterson et al., 1993. Eur J Protistol **34**:369–375

Patterson DJ (1985) The fine structure of *Opalina ranarum* (family Opalinidae): Opalinid phylogeny and classification. Protistologica **21**:413–428

Patterson DJ, Delvinquier BLJ (1990) The fine structure of the cortex of the protist *Protoopalina australis* (Slopalinida, Opalinidae) from *Litoria nasuta* and *Litoria inermis* (Amphibia: Anura: Hylidae) in Queensland, Australia. J Protozool **37**:449–455

Preisig HR (1989) The Flagellar Base Ultrastructure and Phylogeny of Chromophytes. In Green JC, Leadbeater BSC, Diver WL (eds) The Chromophyte Algae: Problems and

Perspectives. Clarendon Press, Oxford, pp 167–187

Riisberg I, Orr RJ, Kluge R, Shalchian-Tabrizi K, Bowers HA, Patil V, Edvardsen B, Jakobsen KS (2009) Seven gene phylogeny of heterokonts. Protist **160**:191–204

Ronquist F, Huelsenbeck JP (2003) MRBAYES 3: Bayesian phylogenetic inference under mixed models. Bioinformatics **19**:1572–1574

Sato T (1968) A modified method for lead staining of thin sections. J Electron Microsc **17**:158–159

Stamatakis A (2006) RAxML-VI-HPC: maximum likelihood-based phylogenetic analyses with thousands of taxa and mixed models. Bioinformatics **22**:2688–2690

Takishita K, Miyake H, Kawato M, Maruyama T (2005) Genetic diversity of microbial eukaryotes in anoxic sediment around fumaroles on a submarine caldera floor based on the small-subunit rDNA phylogeny. Extremophiles **9**:185–196

Vørs N (1992) Heterotrophic amoebae, flagellates and heliozoa from the Tvärminne area, Gulf of Finland, in 1988–1990. Ophelia **36**:1–109

Yabuki A, Inagaki Y, Ishida K (2010) *Palpitomonas bilix* gen. et sp. nov.: a novel deep-branching heterotroph possibly related to Archaeplastida or Hacrobia. Protist **161**:523–538

Yubuki N, Leander BS, Silberman JD (2010) Ultrastructure and molecular phylogenetic position of a novel phagotrophic stramenopile from low oxygen environments: *Rictus lutensis* gen. et sp. nov. (Bicosoecida, incertae sedis). Protist **161**:264–278

Figure 1. Light and transmission electron micrographs of *Platysulcus tardus* gen. nov., sp. nov. AF, anterior flagellum; PF, posterior flagellum. White arrowheads indicate the ventral furrow. The double arrowhead indicates the tubular shaft. The triple arrowhead indicates the terminal filament. **A–E.** Differential interference contrast (DIC) micrographs of hapantotype. Scale bar = 10 μm. **F.** Whole-mount transmission electron micrograph. Scale bar = 2 μm. **G.** High magnification view of the anterior flagellum. Scale bar = 1 μm. **H.** High magnification view of a flagellar hair. Scale bar = 200 nm.

Figure 2. Transmission electron micrographs of *Platysulcus tardus* gen. nov., sp. nov. Ex, extrusome; Fv, food vacuole; G, Golgi apparatus; Mt, mitochondrion; Mb, microbody; N, nucleus; n, nucleolus. Arrows indicate the large flat vesicle. Double arrows indicate the transitional plate. Arrowheads indicate the electron-dense material in the basal body. Asterisks indicate thin fibrous materials. **A.** General cell image of *P. tardus*. Scale bar = 1 μm. **B.** High magnification view of endoplasmic reticulum (ER) including fibrous material. Scale bar = 500 nm. **C.** High magnification view of the nucleus and the microbody. Scale bar = 500 nm. **D.** High magnification view of food vacuoles. Scale bar = 500 nm. **E.** High magnification view of extrusomes. Scale bar = 500 nm. **F.** High magnification view of longitudinal section of the basal body. Scale bar = 200 nm. **G.** High magnification view of cross-section of the proximal part of the basal body. Scale bar = 200 nm. **H.** High magnification view of cross-section of the middle part of the basal body. Scale bar = 200 nm. **I.** High magnification view of cross-section of the transitional region. Scale bar = 200 nm. **J.** High magnification view of cross-section of the proximal end of the flagellum. Scale bar = 200 nm.

Figure 3. Selected serial sections of *Platysulcus tardus* gen. nov., sp. nov. taken from

anterior to posterior. AF, anterior flagellum; Ex, extrusome; Mt, mitochondrion; PB, posterior basal body; PF, posterior flagellum. S, S tubule; R1, root 1; R3, root 3. Scale bar = 500 nm.

Figure 4. Selected serial sections of *Platysulcus tardus* gen. nov., sp. nov. taken from anterior to posterior. Ex, extrusome; Fv, food vacuole; Mt, mitochondrion; PF, posterior flagellum. S, S tubule; R1, root 1; R2, root 2. Arrows indicate the large thin vesicle. Scale bar = 500 nm.

Figure 5. Selected serial sections of *Platysulcus tardus* gen. nov., sp. nov. taken from dorsal to ventral. AB, anterior basal body; Ex, extrusome; Fv, food vacuole; PB, posterior basal body; PF, posterior flagellum. S, S tubule; R1, root 1; R2, root 2; R3, root 3; R4, root 4. Arrows indicate the large thin vesicle. Scale bar = 500 nm.

Figure 6. Illustration of the microtubular roots of *Platysulcus tardus* gen. nov., sp. nov. AB, anterior basal body; PB, posterior basal body; S, S tubule; R1, root 1; R2, root 2; R3, root 3; R4, root 4.

Figure 7. Maximum-likelihood tree of 103 stramenopiles, 5 rhizarians, and 5 alveolates using 1,607 positions of the small subunit (SSU) rRNA gene. Environmental sequences were labeled with accession numbers. Only bootstrap probability ≥50% is shown. Nodes supported by Bayesian posterior probabilities ≥0.98 are highlighted by bold lines.

Fig. 1

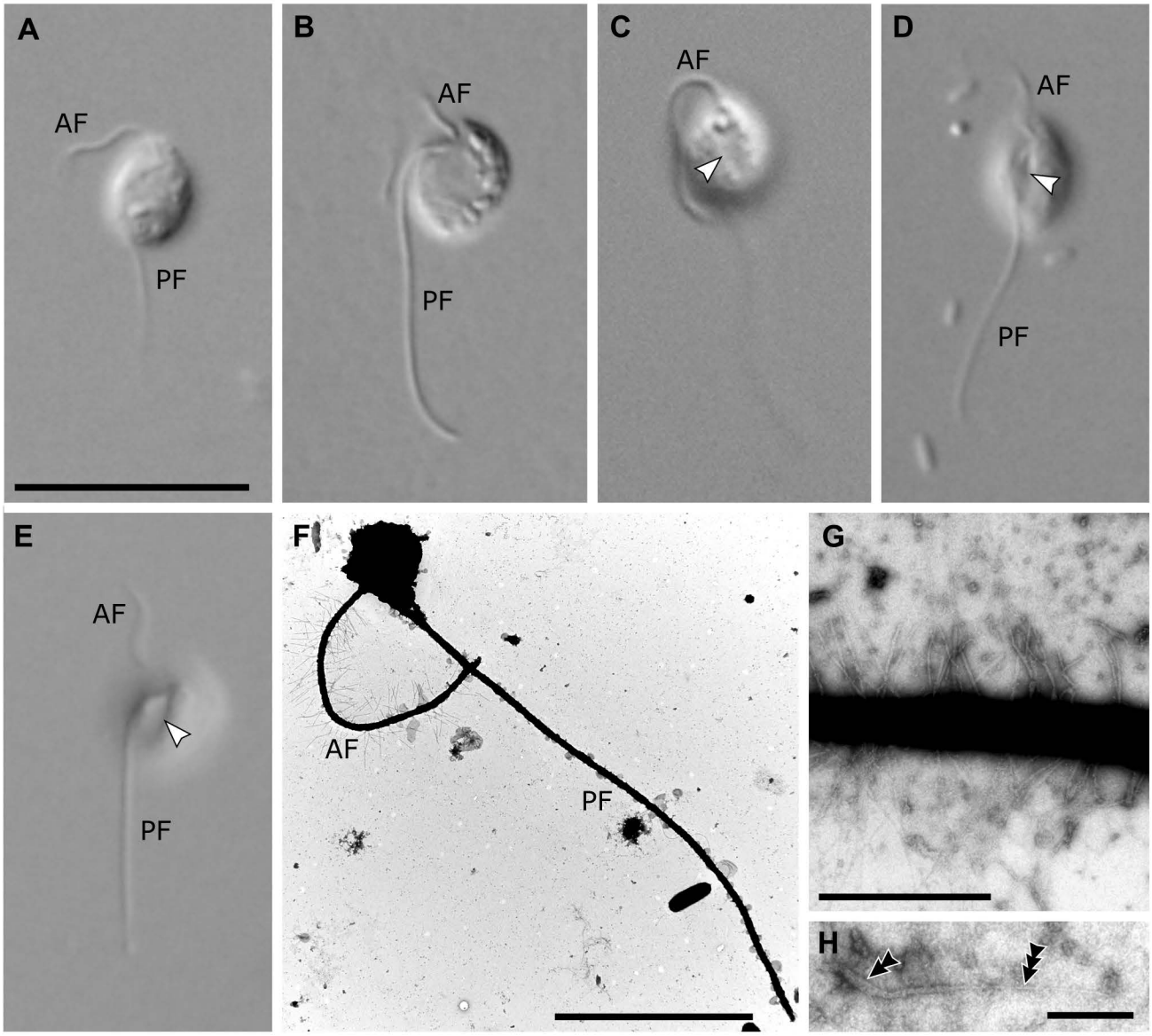

Fig. 2

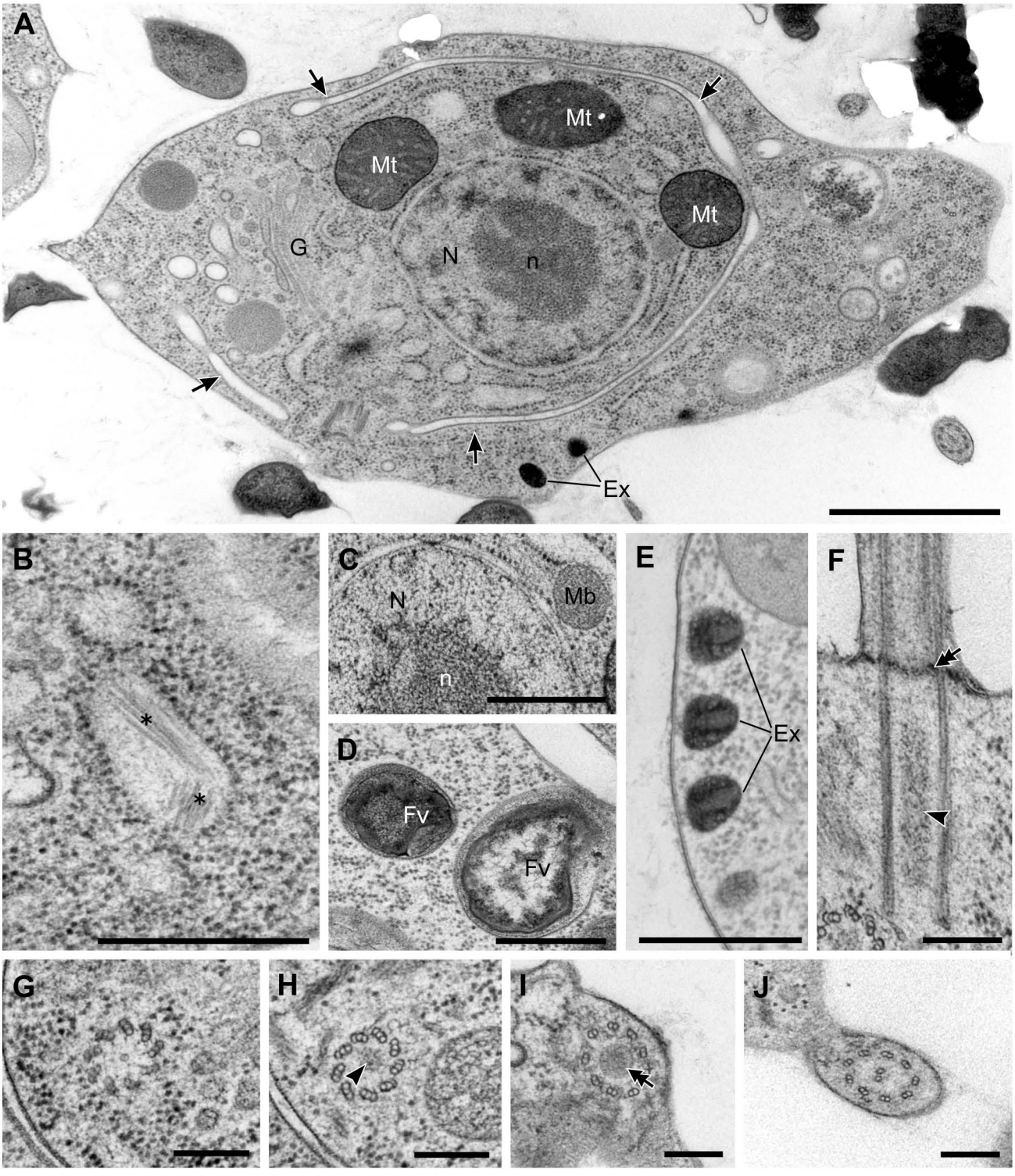

Fig. 3

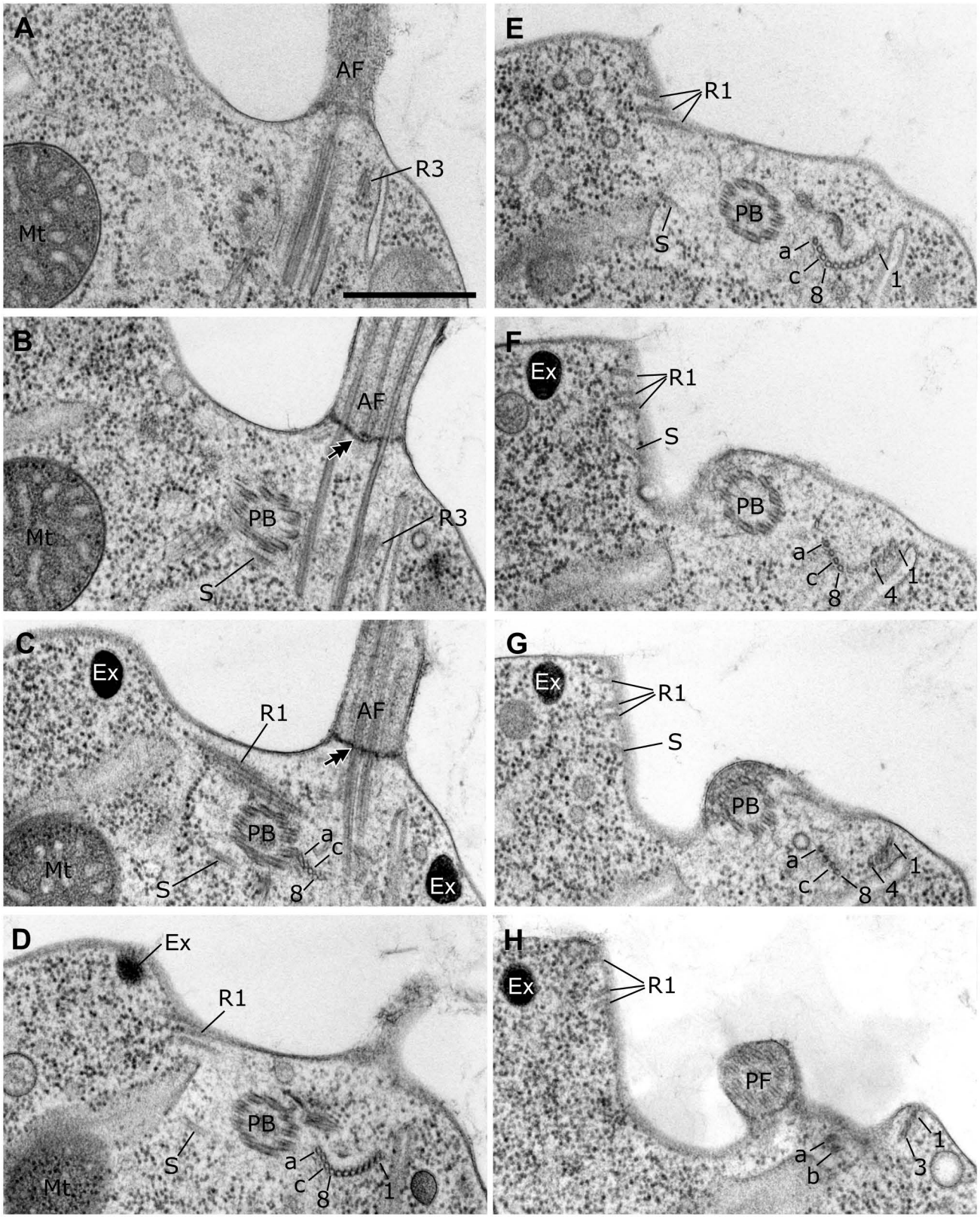
A
AF
R3
Mt
E
R1
PB
S
a
c
8
1
B
AF
PB
R3
Mt
S
F
Ex
R1
S
PB
a
c
8
4
1
C
Ex
R1
AF
PB
a
c
Mt
S
8
Ex
G
Ex
R1
S
PB
a
c
8
4
1
D
Ex
R1
PB
S
a
c
8
1
Mt
H
Ex
R1
PF
a
b
3
1

Fig. 4

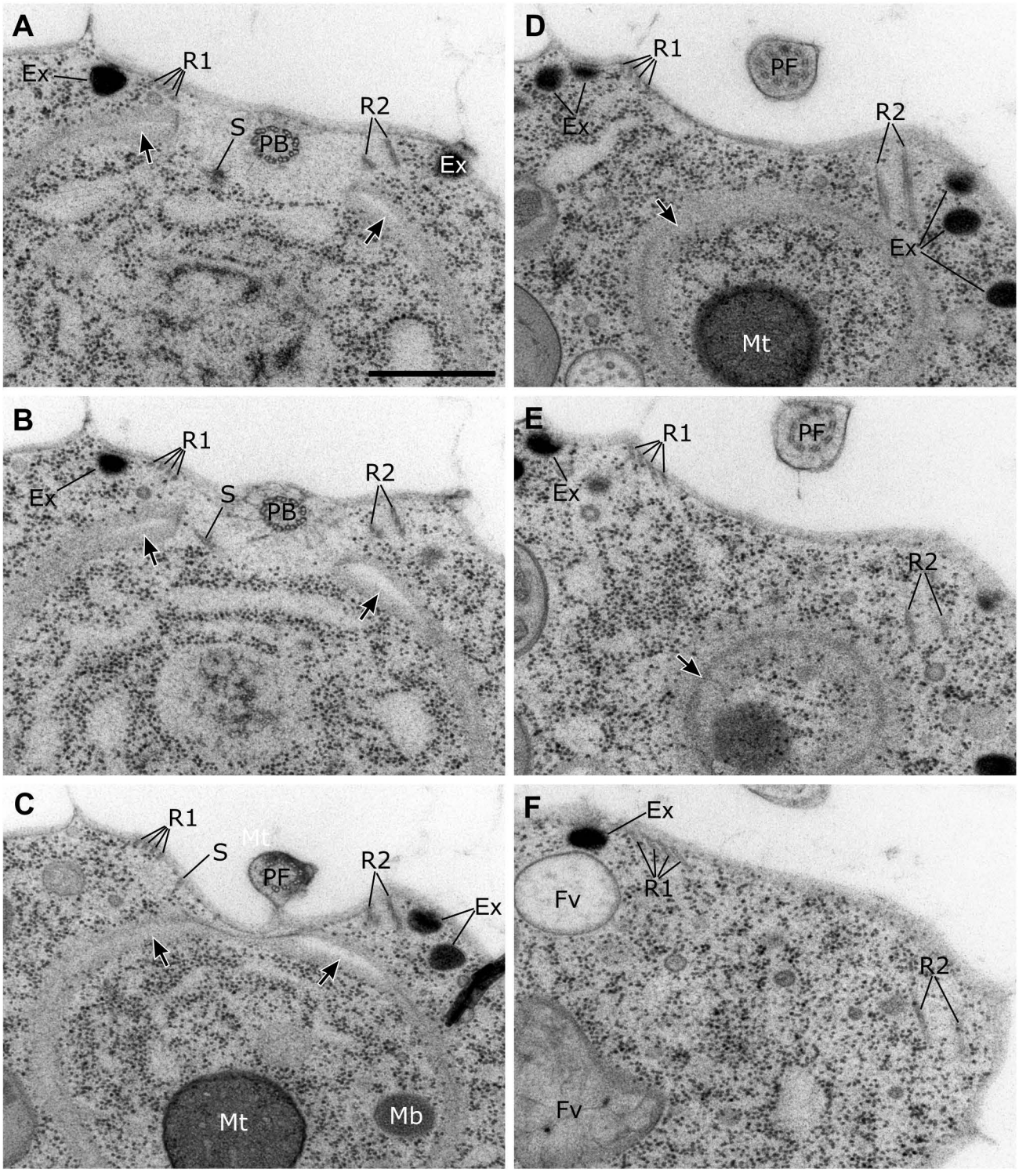
A
Ex
R1
S
PB
R2
Ex
B
Ex
R1
S
PB
R2
C
R1
S
Mt
PF
R2
Ex
Mt
Mb
D
R1
PF
Ex
R2
Ex
Mt
E
R1
PF
Ex
R2
F
Ex
R1
Fv
R2
Fv

Fig. 5

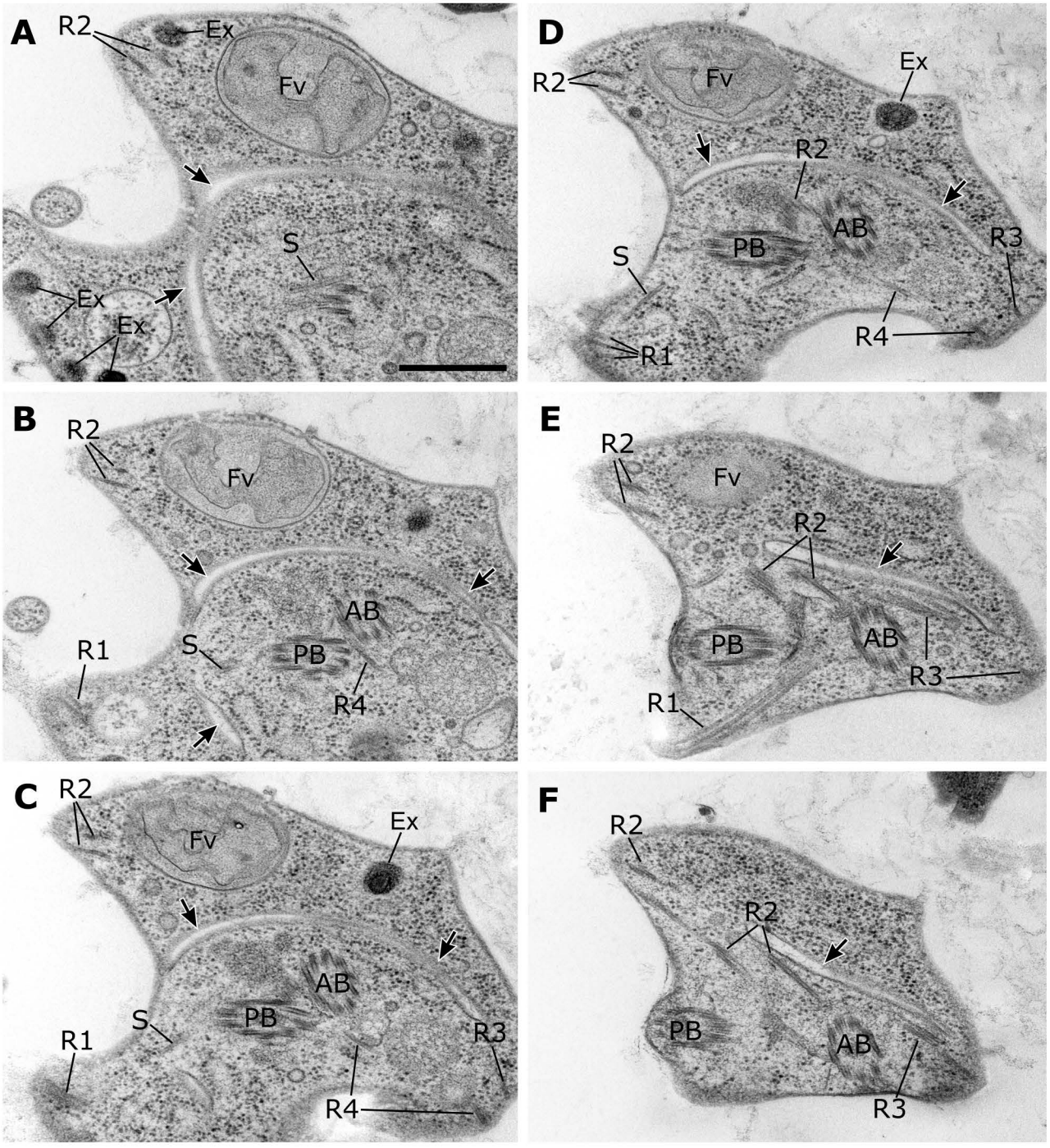
A
R2
Ex
Fv
S
Ex
Ex
D
R2
Fv
Ex
R2
AB
PB
S
R3
R4
R1
B
R2
Fv
AB
R1
S
PB
R4
E
R2
Fv
R2
PB
AB
R3
R1
C
R2
Fv
Ex
AB
PB
S
R1
R3
R4
F
R2
R2
PB
AB
R3

Fig. 6

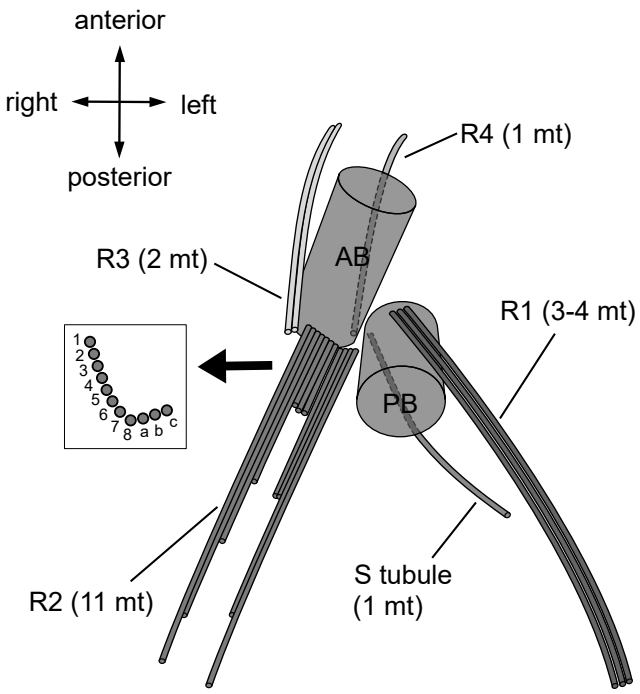
anterior
right
left
posterior
R4 (1 mt)
R3 (2 mt)
AB
R1 (3-4 mt)
1
2
3
4
5
6
7
8
a
b
c
PB
R2 (11 mt)
S tubule
(1 mt)

Fig. 7


Tribonema aequale M55286
Heterococcus caespitosus AF083399
Xanthophyceae
Fucus gardneri X53987
Phaeophyceae
Schizocladia ischiensis AB085614
Schizocladiophyceae
Heterosigma akashiwo U41650
Raphidophyceae
Pelagomonas calceolata U14389
Aureoumbra lagunensis U40258
Pelagophyceae
Pinguiococcus pyrenoidosus AF438324
Pinguiophyceae
Nannochloropsis salina M87328
Eustigmatophyceae
Ochromonas danica M32704
Oikomonas mutabilis U42454
Mallomonas striata M87333
Chrysophyceae
Synchroma grande DQ788730
Synchromophyceae
Ciliophrys infusionum L37205
Pseudopedinella elastica U14387
Dictyocha speculum U14385
Dictyochophyceae
Ochrophyta
Bolidomonas pacifica AF167157
Triparma sp. AB546639
FJ032657
Bolidophyceae
Skeletonema costatum x52006
Nitzschia apiculata M87334
Rhizosolenia setigera M87329
Bacillariophyceae
Pirsonia punctigera AJ561115
Pirsoniida
Rhizidiomyces apophysatus AF163295
Hyphochytrea
Achlya bisexualis M32705
Phytophthora megasperma M54938
Olpidiopsis sp. AB363063
Oomycetes
AJ402350
AF363191
MAST-1
GU823473
GU823453
MAST-23
Develpayella elegans U37107
Bigyromonadea
AF363186
AF290083
MAST-2
Blastocystis hominis U51151
Blastocystis cycluri AY266474
Blastocystis sp. DQ186645
Blastocystis geocheloni AY266473
Blastocystea
Karotomorpha sp. DQ431242
Protoopalina intestinalis AY576544-6
Slopalinea
Proteromonas lacertae U37108
AB275092
AF372755
AB275040
EF219382
AF167414
MAST-12
AB275039
AY381200
Solenicola setigera HM163291
Incisomonas marina JN848814
AY381204
AJ402357
EU446323
Nanomonadea
(MAST-3)
Wobblia lunata AB032606
Placidia cafeteriopsis AB061218
Placididea
GU825372
AY256308
MAST-21
Adriamonas peritocrescens AF243501
Siluania monomastiga AF072883
Paramonas globosa AY520452
AY919697
Filos agilis FJ971856
Nerada mexicana AY520453
Cafeteria roenbergensis L27633
AY129062
Caecitellus parvulus AY520457
Halocafeteria seosinensis DQ269470
Bicosoeca vacillans AY520445
DQ103795
Bicosoeca petiolata AY520444
EU446304
Pseudobodo tremulans AF315604
Rictus lutensis GQ223284
Bikosea
GU823104
GU823089
MAST-16
HM749939
AB505495
MAST-24
EF526900
EF526979
AB505560
MAST-22
GU825694
AF363207
MAST-6
AF363188
AF363189
MAST-4
AY381196
MAST-11
EF539114
EU500081
MAST-25
AY129064
AY381191
AJ402355
MAST-7
AY381186
AY381181
MAST-8
AY381217
AB191426
AB275041
MAST-9
AY295587
MAST-10
Aplanochytrium kerguelense AB022103
Labyrinthula sp. AF348522
Thraustochytrium aureum AB022110
Labyrinthulea
AY256309
MAST-20
Platysulcus tardus gen. nov., sp. nov.
STRAMENOPILES
Prorocentrum micans M14649
Alexandrium tamarense X54946
Toxoplasma gondii M97703
Theileria buffeli AF236094
Onychodromus quadricornutus X53485
ALVEOLATA
Cercomonas longicauda DQ442884
Tremula longifila HQ121439
Platyreta germanica AY941200
Gromia oviformis AJ457814
Sticholonche sp. AY268045
RHIZARIA
0.1
0.4